Studies on Behaviour of in Service Tubular Material Used at Refinery Process Furnaces

IBRAHIM NAIM RAMADAN, EUGEN VICTOR LAUDACESCU, MARIA POPA, LOREDANA IRENA NEGOITA*
Petroleum-Gas University of Ploiesti, 39 Bucharest Blvd, 100680, Ploiesti, Romania

The purpose of the heat transfer analysis at the level of the technological furnace in radiation section was to determine the medium temperature on the outside wall of the pipeline through which the effluent is processed. It is important to keep an outside temperature of the wall of the duct below the maximum allowable temperature at which this carburizing process takes place. Thus, the temperature calculated on the outside pipe wall is 523.5 °C and the maximum allowable temperature of the outside pipe wall is 595.5°C. The carburizing process leads to the modification of the thermal conductivity of the tubing material. Therefore, if steel is enriched with carbon, thermal conductivity decreases.

Keywords: refinery furnaces, heat transfer, steel carburization, tubular material, thermal conductivity

The most important degradation phenomenon is creep, it having the highest rate in tubular material failure. According to API 579, creep intensity increases with temperature over the creep exclusion temperature, below which creep effects are negligible. Also, the loads to which tubular material is exposed during operation, can gain varying loads character, when temperature and pressure fluctuations are large and over degradation effects due to creep its combine with destructive effects of fatigue.

Carburization and oxidation phenomena, also specific to tubular coils, due to circulated technological fluids through coils and the atmosphere inside the furnace, have secondary role in degradation of pipes, as there is thermal controlling possibility, materials with good characteristics regarding creep and fatigue resistance selection and the use of inhibitors [1, 2].

The technological fluid consists of a mixture of hydrocarbons flowing inside tubes, is a carburizing environment, which produces inside carburization of pipes and the atmosphere inside the furnace produces superficial oxidation and/or decarburization on the outside surface of tubes. Carburizing involves carbides formation in the metallic material, as a result of a high carbon content atmosphere exposure. Prolonged exposure leads to loss of mechanical properties [1-3].

In the technological processes inside furnaces, due to high temperatures and technological fluids circulated through coils, the carbon clogs on the internal surface, forming coke, which must be constantly removed, because it may not produce changes of the mechanical properties. On the internal surfaces, an oxide scale (Cr_2O_3, Al_2O_3) is formed, that inhibits the passage of carbon in the metallic material. The carbon is not soluble in chromium, and can penetrate the metallic wall just by diffusion of molecules passing through cracks or pores in the protective layer formed on the surface of tubular material. In normal operating conditions, the formed oxide scale presents defects, due to degradation by creep and to pipe decoking procedures, which makes the carbon atoms to diffuse into the pipe surface through discontinuous zones formed on the surface of tubes [1, 2, 4].

The increase of steel pipe carbon percentage, determined by inside carburization, due to carbon diffusion from technological fluid in pipe wall, will determine thermal conductivity decrease [1]. In the following, the variation of thermal conductivity, λ, with temperature change will be demonstrates.

Technical Conditions of the Tubes

The tube parameters in the furnace radiation section at the catalytic reforming plant in refinery are outside diameter, D_o = 91 mm and wall thickness, δ_w = 8 mm and the pipes are made of P91 (9Cr1MoV) stainless steel. The operated furnace was functional for a period of 344 days and has not been use 55 days due to regular technical revisions. Data representing operating conditions found in the figures 1 and 2, excluding temperatures whose values are below the minimum needed to produce the phenomenon of creep. Thus, in figures 1 and 2, the sequence of a) were taken for the abscissa the intervals shown in the table 1, and the sequence b), were cumulatively these ranges [5].

Table 1

TEMPERATURE - OPERATING UNEQUAL TIME INTERVALS

Hours	24	48	72	96	120	168	192	288	336	384	408	648	744	864	744	864	1200	1344
Number of hourly intervals	15	1			3	1												

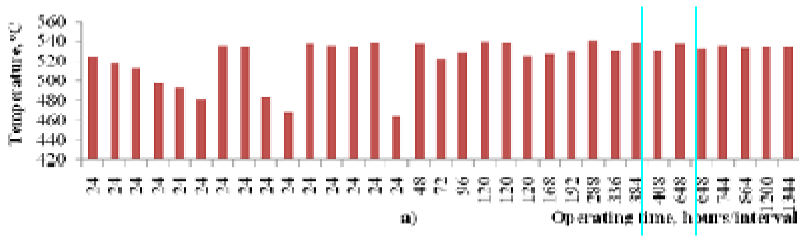

Fig. 1a. Histogram: temperature - operating unequal time intervals

* email: irena.negoita@gmail.com

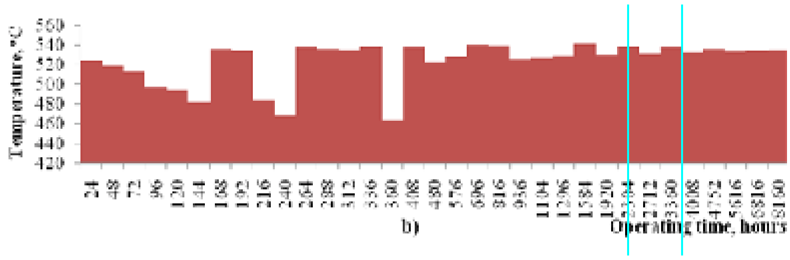

Fig. 1b. Histogram: temperature - operating unequal cumulated time intervals

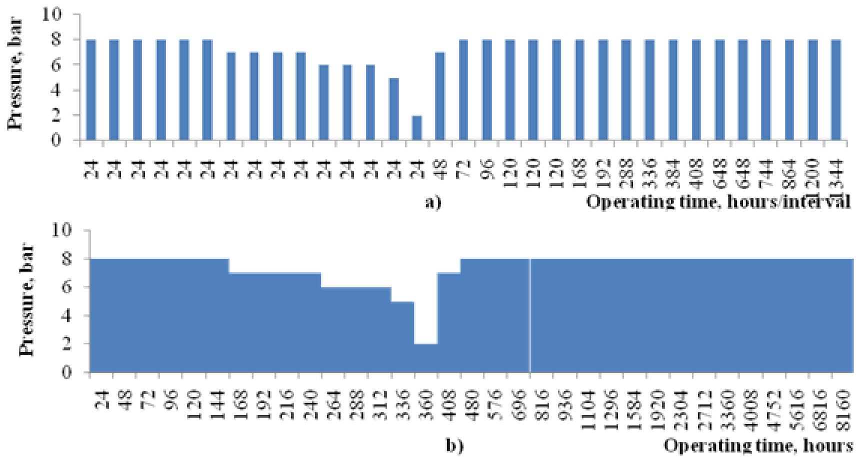

Fig. 2. Histogram: a) pressure - operating unequal time intervals; b) pressure - operating unequal cumulated time intervals

In figure 3 the inside and outside surfaces of furnace tubes can be seen. The analysis of some metallic samples of the tubes was performed on a Scanning Electronic Microscope (SEM). It can be seen that the cementite layer disintegrates, resulting in particles catalyzing the coke deposit on the surface of the steel tubes. Initially, on the surface, small scattered pitting sites were present, which united due to continuous exposure to the working environment, finally causing generalized degradation of steel.

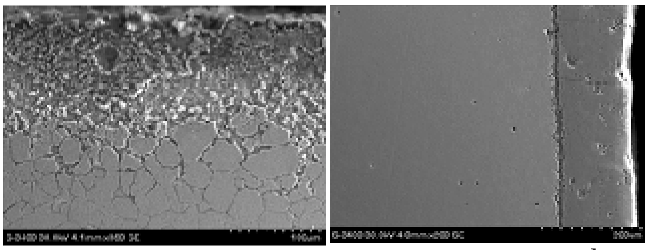

Fig. 3. Images obtained after the microscopic examination of the tubes from H1 furnace: a) inner surface; b) outer surface

Tubular material hardness test

The Vickers hardness test is regulated by [6], and uses a square-based pyramid diamond indenter with the faces set at a 136 ° degree angle from one another. Schematic representation of Vickers hardness test is shown in figure 4 [7].

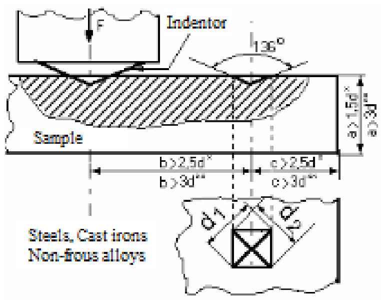

Fig. 4. Schematic representation of Vickers hardness test [7]

In order to determine the hardness of metallic materials, a pyramid diamond indenter is pressed, a certain time τ_d (τ_d = 10...35 s), with a force *F*, on a sample of tested material and after passage of time τ_d, the penetrator is removed and both diagonals, d_1, d_2, are measured, in order to determine their arithmetic average [7]:

$$d = \frac{d_1 + d_2}{2} \quad (1)$$

For hardness determination, the arithmetic average of three values obtained on samples tested on a hardness testing machine was made for each of the distances along the thickness, from inside to outside of the tubes. The assessing hardness values accuracy was performed using Youden diagram [8, 11]. As it can be seen in table 2, the hardness values of the samples from the three technological furnaces, H1, H2, H3, in the catalytic reforming plant have significantly higher values than the unused (new) tube.

The effluent (hydrofined gasoline and a recirculated gaseous mixture), at high temperatures, favors the passage of carbon by diffusion from the working environment in the tube surface. Because of the carburizing process from inside of tubes, hardness values are slightly higher at the inside of the tubes.

Tubular material chemical composition test

The determination of chemical composition was made on the same samples as for hardness testing using Optical Emission Spectroscopy principle; the arithmetic average of three obtained values was made, both on the inside and on the outside of the tubes.

Optical Emission Spectroscopy works by exciting atoms with energy produced by a spark formed between an electrode and the sample. This energy makes electrons from the sample to emit light that is processed into a spectral pattern. By measuring the intensity of the spectrum, the analyzer indicates the chemical compositions of the samples.

As can be seen from tables 3 and 4, the chemical compositions, determined on the samples taken from the steel tubes are in accordance with the stipulations of standard [9].

Table 2
HARDNESS VARIATION OF STEEL TUBES

Distance measured by thickness* [mm]	Hardness values, HV5, [HV]				
	H1 (pipe)	H1 (elbow)	H2 (pipe)	H3 (pipe)	H3 (elbow)
0,25	488	552	236	528	541
0,30	475	537	235	524	528
0,35	456	522	234	517	516
0,40	432	517	233	506	512
0,45	427	494	232	503	503
0,50	433	487	231	501	497
0,55	431	478	235	494	493
0,60	432	462	236	476	481
0,70	427	442	234	459	474
0,75	424	424	241	447	461
0,80	423	423	235	435	450
0,85	422	423	234	429	442
0,90	419	421	235	426	436
1,00	418	420	237	421	431
1,25	417	418	234	417	428
1,50	415	416	236	412	423
1,60	414	412	237	411	418
2,00	412	405	238	407	403
2,50	413	407	234	395	396
3,00	411	400	236	396	389
4,00	409	398	239	392	387
5,00	408	397	233	389	384
6,00	406	396	234	387	384
7,00	407	394	236	389	383

* from the inside to the outside of the pipe

Table 3
CHEMICAL COMPOSITION OF H1, H2 AND H3 FURNACE TUBES SAMPLES

Chemical elements	H1 (pipe), mass %		H1 (elbow), mass %		H2, mass %		H3 (pipe), mass %		H3 (elbow), mass %	
	outside	inside	outside	inside	outside	inside	outside	inside	outside	inside
C	0.094	0.214	0.0687	0.189	0.06335	0.04685	0.095	0.128	0.1	0.162
Si	0.292	0.294	0.297	0.299	0.3715	0.349	0.676	0.667	0.771	0.6645
Mn	0.517	0.506	0.524	0.513	0.5235	0.4965	0.564	0.51	0.507	0.504
P	0.0201	0.0166	0.0181	0.0146	0.0064	0.0085	0.0176	0.0148	0.0196	0.0174
S	0.0025	0.0017	0.0015	0.0007	< 0.0005	< 0.0005	0.0073	0.0058	0.0083	0.0072
Cr	9.32	9.27	9.22	9.17	9.585	9.455	9.75	9.7	9.85	9.705
Mo	0.893	0.88	0.918	0.905	0.953	0.904	0.997	0.981	0.972	0.949
Ni	0.171	0.172	0.121	0.122	0.3905	0.2755	0.181	0.13	0.231	0.178
Al	0.0093	0.0093	0.0088	0.0088	0.0098	0.0103	0.0139	0.013	0.0144	0.0137
Nb	0.0126	0.0119	0.0126	0.0119	0.06205	0.05095	0.0089	0.0137	0.0089	0.01155
V	0.0324	0.0301	0.0237	0.0231	0.2365	0.2265	0.0181	0.0183	0.0191	0.0194
N	0.0956	0.124	0.0906	0.119	0.0325	0.028	0.0731	0.0676	0.0781	0.07785

Table 4
CHEMICAL COMPOSITION OF X10CRMOVNB9-1 STEEL, ACCORDING TO [8]

Chemical elements	C	Si	Mn	P	S	Cr	Mo	Ni	Al	Nb	V	N
Mass %	0.08 - 0.12	max 0.5	0.3 - 0.6	max 0.025	max 0.015	8 - 9.5	0.85 - 1.05	max 0.4	max 0.03	0.06 - 0.1	0.18 - 0.25	0.03 - 0.07

Analyzing the percent concentration of tube steels (table 3) an increasing carbon concentration inside the tubular material was observed, which reflects the carburizing phenomena.

The calculation of the outside temperature of the pipe wall from the radiation section in catalytic reforming furnace

The case study aims to determine the outside temperature of the wall pipes in the radiation section at a technological furnace in the catalytic reforming plant. Temperature changes will modify the thermal conductivity of the tubing material. Study of heat transfer through cylindrical simple walls or/and cylindrical compound walls, involves calculations for determining the temperatures of the wall, taking into account the working fluid temperatures [12, 13]. To highlight the effect of carburization on the tubular material, a study was carried out on heat transfer to U-shaped tubes in the furnace of the radiation section of the catalytic reforming plant in a petroleum refinery.

Their main geometric features are shown in figure 5.

The raw material, effluent, consists of a mixture of hydrofined gasoline and recirculated gases (this gaseous mixture contain about 87 % vol. H_2, 6% vol. CH_4, 4 % vol. C_2H_6 and 3 % vol. other gaseous hydrocarbons). The main design features of the tubes and the effluent properties are shown in table 5.

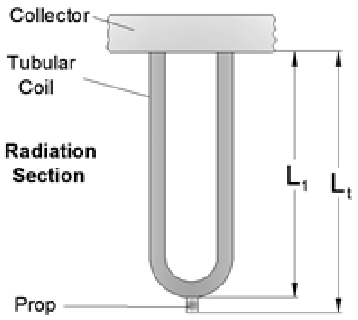

Fig. 5. Schematic representation of tubular coils (U tubes in furnace radiation section)

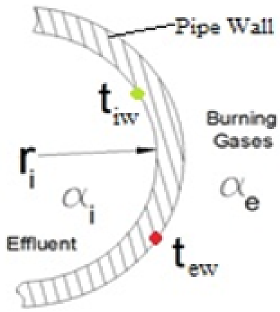

Fig. 6. Schematic diagram of heat transfer effect

Table 5
MAIN GEOMETRICAL PARAMETERS OF THE TUBES AND THE EFFLUENT PHYSICAL PROPERTIES

Parameters	Symbol	Value	UM
Tube outside diameter	D_e	91	mm
Tube inside diameter	D_i	75	
Tube wall thickness	δ_w	8	
Tube length	L_1	12.755	m
Total length (coil and prop)	L_t	13.12	
Total tubes number	n_t	24	-
Inlet temperature of the effluent	t_i	460	°C
Outlet temperature of the effluent	t_o	529	
Medium temperature of the effluent	$\overline{t_m}$	494.5	
Temperature difference between inlet and outlet temperatures of the effluent	Δt	69	°C
Inside surface area of the coil	A_i	144.3	m^2
Outside surface area of the coil	A_o	175	
Necessary heat flow of the effluent	Q	4.278	kW
Flow rate of the effluent	m	14.12	kg/s
Effluent density	ρ	3.27	kg/m^3
Effluent specific heat	c_p	3.748.5	J/(kg·°C)
Effluent dynamic viscosity	μ	$0.027 \cdot 10^{-3}$	kg/(m·s)
Effluent thermal conductivity	λ	0.1986	W/(m·°C)

Table 6
VALUES OF THE CALCULATED PARAMETERS

Parameters	Symbol	Value	UM
Velocity of fluid	w	40.75	m/s
Reynolds number	Re	364.1	-
Prandtl number	Pr	0.518	-
Nusselt number	Nu	610	-
Inner heat transfer area	A_i	144	m^2
Inner convective heat transfer coefficient	α_i	1.315	W/(m^2·°C)
Inner wall temperature	t_{iw}	517	°C
Outside wall temperature	t_{ow}	523.5	°C
Medium temperature between fluids	t_{mf}	520.25	°C
The thermal conductivity for steel	λ_{steel}	33.2	W/(m·°C)
Outside heat transfer area	A_e	175	m^2
Temperature of the flue gases	$t_{flue\ gases}$	750	°C
Outside convective heat transfer coefficient	α_o	108	W/(m^2·°C)
Global heat transfer coefficient	k_e	96	W/(m^2·°C)
Thermal tension	T_t	24.441	W/m^2
Maximum thermal tension	$T_{t\ max}$	56.017	W/m^2
Global heat transfer coefficient between the feedstock and external surface	$k_{f\text{-}ow}$	842	W/(m^2·°C)
Maximum temperature on the outside pipe wall	t_{ow}^{max}	595.5	°C
The new thermal conductivity for steel	$\lambda_{steel\ new}$	32.6	W/(m·°C)

Velocity of fluid inside the pipes is calculated with the relation [10]:

$$w = \frac{m}{\rho \frac{\pi D_i^2}{4} \cdot n_t}, \text{ m/s} \quad (2)$$

For the calculation of partial heat transfer coefficients (a), the relation 3 [10] is used

$$Nu = 0.023 \cdot Re^{0.8} \cdot Pr^{0.4} \quad (3)$$

where:

$$Re = \frac{D_i \cdot w \cdot \rho}{\mu} \quad (4)$$

$$Pr = \frac{c_p \cdot \mu}{\lambda} \quad (5)$$

$$Nu = \frac{\alpha_i \cdot D_i}{\lambda} \quad (6)$$

The inner wall temperature, t_{iw} was determined with the following formula [10]:

$$Q = \alpha_i \cdot A_i (t_{iw} - \bar{t}_m), \quad (7)$$

Where Q is heat transfer flow and this was calculated with the formula listed below,

$$Q = m \cdot c_n \cdot \Delta t$$

$$A_i = \pi \cdot Di \cdot L_1 \cdot n_t, \text{ m}^2 \quad (8)$$

The Fourier law applied for the cylindrical wall (figure 6) is given by the following expression (9):

$$Q = \frac{2\pi \cdot n_t \cdot L_1 (t_{ow} - t_{iw})}{\frac{1}{\lambda_{steel}} \ln \frac{D_o}{D_i}} \quad (9)$$

If the medium temperature in the heating chamber is known, it is possible to calculate α_o (on the combustion gas side) using the following relation [10]:

$$Q = \alpha_o \cdot A_o \left(\bar{t}_{flue\ gases} - t_{ow}\right) \quad (10)$$

$$A_o = \pi \cdot D_o \cdot L_1 \cdot n_t \quad (11)$$

The thermal conductivity was calculated after a variation of shape [10]:

$$\lambda_{steel} = 37.4 - 0.008 \cdot t \quad (12)$$

The global heat transfer coefficient was calculated using the expression [10]:

$$k_e = \frac{1}{\frac{D_o}{\alpha_i \cdot D_i} + \frac{D_o}{2\lambda_{steel}} \ln \frac{D_o}{D_i} + \frac{1}{\alpha_o}} \quad (13)$$

Thermal tension in the radiation section will be determined [10]:

$$T_{tR} = \frac{Q}{A_o} \quad (14)$$

Maximal allowable thermal tension will be determined with [10]:

$$T_{thermal}^{max\,allowable} = C_1 \cdot C_2 \cdot C_3 \cdot T_t \quad (15)$$

where, C1=1.93, C2=1.25, C3=0.95 [10]

The maximum value of temperature on the outside pipe wall is [10]:

$$t_{ow}^{max} = t_{effluent}^{max} + \frac{T_{term}^{maxadm}}{k_{f-ow}} \quad (16)$$

where $k_{f\text{-}ow}$ is the global heat transfer coefficient between the feedstock and outside surface of pipe walls and is calculated with [10]:

$$k_{f\text{-}ow} = \frac{1}{\frac{D_o}{\alpha_i \cdot D_i} + \frac{D_o}{2\lambda_{steel}} \ln \frac{D_o}{D_i}} \quad (17)$$

As will be seen, increasing the wall temperature will reduce the thermal conductivity.

Based on relationships (2)-(17), the results for the calculated sizes are shown in table 6.

Conclusions

Structural changes during exploitation refer to alloying elements, that are distributed at grain boundaries or inside the ferritic or austenitic matrix: carbides, nitrides or carbonitrides (of alloying elements) and intermetallic compounds, due to diffusion of carbon excess on the inside walls of pipes.

Assessment of technical condition of coils by mechanical and technological tests carried out with periodic revisions involves specific procedures in order to be able to determine any changes resulting from exploitation, for different periods of time;

The paper only refers to tubular material components without defects, but in many cases, they may have indentations due to manipulation or accidental mechanical contacts.

It is important to keep an outside temperature of the wall of the duct below the maximum allowable temperature at which this carburizing process takes place. Thus, the temperature calculated on the outside pipe wall is 523.5 °C and the maximum allowable temperature of the outside pipe wall is 595.5 °C. The carburizing process leads to the modification of the thermal conductivity of the tubing material. Therefore, if steel is enriched with carbon, thermal conductivity decreases.

The increase of outside wall temperature of the pipe near or above the permissible maximum temperature shows that the carburizing process takes place at the level of the pipes in the furnace radiation section.

References

1. GRABKE, H.J., Materiali in Tehnologije, **36**, Max-Planck-Institut für Eisenforschung GmbH, Düsseldorf, 2002, p. 297

2. RAMADAN, I. N., Studies about Increasing the Service Life of Tubular Material from Furnaces in Refineries and Petrochemical Plants**,** PhD Thesis, Petroleum-Gas University of Ploiesti, September 2016

3. A. J. M. H. HABEEB, N. N. ANTONESCU, M. G. PETRESCU, Journal of the Balkan Tribological Association, **21**, no. 4, 2015, p. 842

4. NATESAN, K., ZENG, Z., MARONI, V.A., SOPPET, W.K., RINK, D.L., Metal Dusting Research at Argonne National Laboratory, International Workshop on Metal Dusting, Argonne National Laboratory, S.U.A., 2001, 25 pages

5. NEACSA, A., ANTONESCU, N.N., STOICA, D.B., Journal of the Balkan Tribological Association, **15** (4), 2009, p. 474

6. *** ISO 6507-1:2018, Metallic materials - Vickers hardness test - Part 1: Test method

7. ZECHERU, Gh., DRAGHICI, Gh., Elemente de stiinta si ingineria materialelor, vol. I, ILEX and Petroleum - Gas University of Ploiesti Publishing Houses, 2001

8. DINITA, A., 13TH International Conference on Tribology (ROTRIB'16), IOP Conference Series-Materials Science and Engineering, Volume: **174**, 2017, p. 537

9. *** EN 10216-2, Seamless Steel Tubes for Pressure Purposes. Technical Delivery Conditions. Non-alloy and Alloy Steel Tubes with Specified Elevated Temperature Properties, 2014

10. DOBRINESCU, D., Procese de transfer de caldura si utilaje specifice, Didactic and Pedagogical Publishing House, Bucharest, 1983

11. NEACSA, A., DINITA A., BARANOWSKI, P., SYBILSKI, K., RAMADAN I. N., MALACHOWSKI, J., BLYUKHER, B., Journal of Pressure Vessel Technology - Transactions of the ASME, 138, Issue: 3, 2016, p. 17 (digital collection).

12. POPA, M., ONUTU, I., Rev. Chim. (Bucharest), **60**, no.11, 2009, p.1185

13. PATRASCIOIU, C., NEGOITA, L. (2014). The Convection Heater Numerical Simulation, XII International Conference on Thermal and Fluids Engineering, Venice, International Science Index **8**, No.4, 2014, p. 335

Manuscript received: 7.03.2018